

A crack extension force correlation for hard materials

W. W. Gerberich · W. M. Mook · C. B. Carter ·
R. Ballarini

Received: 13 August 2007 / Accepted: 18 January 2008
© Springer Science+Business Media B.V. 2008

Abstract Increasingly, the essential, robust character of many nanoscale devices requires knowledge of their fracture toughness. For most brittle materials the technique of choice has been indentation mechanics but little insight into the fracture mechanism(s) has resulted since these have generally been treated as brittle fracture dominated by the true surface energy. Linear elastic fracture mechanics approaches have been invoked to describe indentation fracture but do not address why the surface energy from fracture toughness is most often slightly or even substantially greater than the true surface energy. In the present study we invoke a crack extension force correlation that demonstrates why this is the case at least in fracture measurements based on indentation mechanics. The proposed correlation is different from previous ones in that it focuses on observations of indentation-induced dislocation activity prior to fracture. Allowing the resistance side of the crack extension force analysis to incorporate small amounts of plasticity gives a relationship that is consistent with 22 relatively brittle intermetallics, semiconductors and ceramics. This explains why measured strain energy release rates can be 2 to 5 times as large as surface

energies measured in vacuum or calculated by pseudopotentials using the local density approximation.

Keywords Fracture mechanics · Indentation · Dislocation · Fracture toughness · Ceramic materials · Intermetallic materials

Why are fracture toughness and hardness values highly correlated (Veprek and Argon 2002; Yonenaga 2005) in many hard materials? We propose that dislocation activity precedes fracture by indentation in almost all crystalline, single-phase materials in the absence of grain boundary failure. This leads to a correlation function for predicting mode-I or mode-II fracture toughness, K_{Ic} or K_{IIc} , that is validated by independently determined dislocation shielding models (Huang and Gerberich 1992; Li 1986; Lin and Thomson 1986). Previously hardness and fracture toughness correlations were basically linear-elastic fracture mechanics based upon hardness representing a stress and using measured crack lengths. These defined an applied stress intensity which, with a constant, correlated the measured fracture toughness to other measures of fracture toughness (Anstis et al. 1981; Evans and Charles 1976; Lawn and Wilshaw 1975). This says nothing about the resistance side of any fracture toughness relationship. What is new here is invoking a plasticity-based dislocation shielding argument for some of the most brittle of materials undergoing indentation fracture. This is described as a crack extension force on the driving force side and as a crack-tip shielding force on the resistance side.

W. W. Gerberich (✉) · W. M. Mook · C. B. Carter
Department of Chemical Engineering and Materials
Science, University of Minnesota, 151 Amundson Hall,
421 Washington Ave. SE, Minneapolis, MN 55455, USA
e-mail: wgerb@umn.edu

R. Ballarini
Department of Civil Engineering, University of Minnesota,
Minneapolis, MN 55455, USA

In the simplest of terms, the crack extension force at instability is balanced by the total dislocation shielding resistance that is represented by the plastic displacement of the nucleated dislocations. This total resistance can include both the shielding of the indenter tip (a back stress) and the shielding of the crack-tip. Therefore it is possible to estimate fracture toughness using the hardness, H , and indentation modulus, E , values that are routinely determined with nanoindentation. The proposed model is consistent with 22 relatively brittle intermetallics, carbides, nitrides, oxides, silicides, and semiconductors as well as diamond with K_{IC} values less than $8 \text{ MPa m}^{1/2}$.

Given the relatively recent findings that nanoscale structures can be both harder and tougher than their bulk counterparts (Gerberich et al. 2003b, 2006; Yonenaga 2005), there is considerable interest in using intermetallics and semiconductors in photonic and microelectromechanical system (MEMS) applications as structural members (Moody et al. 2006). It is therefore necessary to address the reliability, and thus fracture toughness, of these macroscopically brittle materials at the nanoscale. Recent studies (Veprek and Argon 2002; Yonenaga 2005) have examined the relationship between hardness and fracture toughness of such materials but have not given significant insight as to why such correlations might be appropriate to single crystals. Considerable plasticity by dislocation slip does occur easily in intermetallics (Ghosh 2004) undergoing indentation. However accepting dislocation plasticity for semiconductors, oxides, silicides, and carbides at room temperature is somewhat more difficult to envision. Nevertheless, room temperature dislocation plasticity in single crystal silicon has been observed via TEM images during nanoindentation (Minor et al. 2005). It has also been observed during the TEM-in situ compression of individual silicon nanoparticles preceding cleavage fracture (Deneen Nowak et al. 2007). Additionally there is ample post-mortem TEM evidence in both silicon carbide (Page et al. 1998) and molybdenum disilicide (Boldt et al. 1992) that dislocation activity precedes crack formation in nano- and micro-indentation. In fact, new research shows that dislocation plasticity can emanate from sharp surface contacts at even nano-Newton loads (Cross et al. 2006; Minor 2006), and is more prevalent than previously imagined.

The proposed concept then is that all the materials presented here have dislocation activity. This leads to a

theoretical construct in which the applied crack extension force is resisted by a corresponding force from emitted dislocations. Such dislocation shielding concepts are not new (Burns 1986; Gerberich et al. 2003a; Li 1986), but we are not aware of any attempts by investigators in the intermetallics and ceramics communities to couple these two concepts for extremely brittle materials. For example Lawn and Wilshaw (1975), Evans and Charles (1976), Anstis et al. (1981) among many others found correlations between K_{IC} , E and H , but these required knowledge of the crack lengths involved. The most popular of these correlations quoted in many textbooks is

$$K_{IC} = \frac{\eta (E/H)^{1/2} P}{c^{3/2}} \quad (1)$$

where P is load, c is crack length and $\eta = 0.016$ which is taken to correct for the difference in K_{IC} values measured by indentation versus conventional tension or beam bending methods. The underlying fracture resistance mechanism of the indented material including any possible role of dislocation plasticity is not considered with this analysis. This may be partly due to the unavailability of fracture toughness information until recently (Ghosh 2004; Yonenaga 2005) and partly due to few dislocation studies that have accompanied fracture results obtained by indentation (Boldt et al. 1992; Page et al. 1998). In this theoretical construct, we have attempted to use hardness data taken at relatively low loads so as to measure the yield stress, σ_{ys} , based upon Tabor's general criterion that yield stress is one-third the material's hardness. Additionally, every attempt was made to obtain fracture toughness values from single crystals or large grain polycrystals where indentation-induced cracks were contained within a single grain thus minimizing the likelihood of additional energy dissipation mechanisms such as non-local dislocation activity or unaccounted for microcracking. Furthermore, single crystals with two-phase microstructures common in some intermetallics, such as TiAl, were avoided. As such, data reported represent closely the fracture resistance of single phase, single crystals with relatively low initial dislocation densities.

For the intermetallics, most data come from Ghosh (2004) for Sn-based systems while the semiconductors, nitrides and carbides come from multiple sources mainly assembled by Yonenaga (2005). A range of fracture toughness and hardness values for diamond and, hence, yield strength was obtained from four sources

Table 1 Data for 22 semi-brittle materials are given where E is elastic modulus, μ is shear modulus, ν is Poisson's ratio and b is the Burgers vectors for the most likely slip system

Material	E (GPa)	ν	μ (GPa)	b (nm)	H (GPa)	σ_{ys} (GPa)	τ_{ys} (GPa)	K_{Ic} (MPa m ^{1/2})	$\sqrt{\mu\bar{\sigma}_{ys}b}$ (MPa m ^{1/2})	Reference
AuSn ₄	71	0.312	27.1	0.59	0.5	0.17	0.11	2.5	0.052	1
Al ₆₆ Ti ₂₅ Mn ₉	174	0.108	79	0.284	—	0.32	0.21	3.5	0.085	2
Cu ₆ Sn ₅	97	0.309	37	~ 0.57	3.44	1.15	0.76	2.8	0.156	1
Ni ₃ Sn ₄	118	0.318	44.8	~ 0.60	3.4	1.13	0.75	4.2	0.174	1
NiAl	200	0.31	76	0.288	4	1.38	0.89	5.3	0.168	3–5
Cu ₃ Sn	123	0.319	46.7	0.55	4.22	1.41	0.94	5.7	0.19	1
ZnSe	65	0.28	25.3	0.245	1.1	0.37	0.24	0.9	0.048	6–8
InAs	65	0.33	25.9	0.26	2.63	0.88	0.59	0.3	0.077	8,9
InP	99	0.36	30.2	0.25	4.49	1.5	1	0.44	0.107	8,10
ZnO	161	0.36	50	0.18	4.7	1.57	1.05	0.6	0.119	8
GaAs	123	0.31	41.5	0.245	5.5	1.83	1.22	0.51	0.136	6,11
GaP	147	0.31	49.7	0.236	7.73	2.58	1.72	0.65	0.159	8
Ge	103	0.28	48.9	0.244	7.12	2.37	1.58	0.6	0.168	8
Si	160	0.218	60.5	0.235	12	4	2.67	0.7	0.238	6,8,12,13
GaN	287	0.17	116	0.196	10.2	3.4	2.27	1.10, 0.8	0.278	6,8
MgO	242	0.18	129	0.28	9	3	2	1.2, 2.5	0.329	6,7
MoSi ₂	400	0.15	175	0.293	8.7	2.9	1.93	3	0.386	14,15
AlN	345	0.22	133	0.192	17.7	5.9	3.94	2.9	0.388	8,16
Al ₂ O ₃	393	0.23	170	0.387	28	9.33	6.22	2.5	0.682	6,8
α SiC	430	0.15	192	0.188	33	11	7.34	3.3 3.2	0.63	6,8,17
Diamond	1050	0.072	478	0.252	80, 100	26.7, 35	17.8	5.3	1.79	6,18–21
CVD S.C. diamond	1050	0.072	478	0.252	153	51	34	8	2.48	21

Yield strengths are presented both as the hardness conversion, $H/3$, and as a shear yield, τ_{ys} , of two-thirds σ_{ys} described by Johnson (1987) as the maximum reduced stress criterion. The last column represents the correlation function as described in Fig. 1. Reference numbers refer to: 1—Ghosh (2004); 2—Kumar (1993); 3—Bergmann and Vehoff (1995); 4—Gerberich et al. (2003a); 5—Kitano and Pollock (1993); 6—Drory et al. (1996); 7—Mecholsky et al. (1976); 8—Yonenaga (2005); 9—Louail et al. (2006); 10—Klose et al. (2002); 11—Margevicius and Gumbsch (1998); 12—Gerberich et al. (2006); 13—Gerberich et al. (2003b); 14—Boldt et al. (1992); 15—Wade and Petrovic (1992); 16—Terao et al. (2002); 17—Espinosa et al. (2006); 18—Bates (2006); 19—Drory et al. (1991); 20—Ruoff (1979); 21—Yan et al. (2004)

(Bates 2006; Drory et al. 1991; Ruoff 1979; Yan et al. 2004). Data for 22 semi-brittle materials with K_{Ic} values ranging from 0.3 to 8 MPa m^{1/2} are given in Table 1 (Bates 2006; Bergmann and Vehoff 1995; Boldt et al. 1992; Drory et al. 1996, 1991; Espinosa et al. 2006; Gerberich et al. 1993, 2003b, 2006; Ghosh 2004; Kitano and Pollock 1993; Klose et al. 2002; Kumar 1993; Louail et al. 2006; Margevicius and Gumbsch 1998; Mecholsky et al. 1976; Ruoff 1979; Terao et al. 2002; Wade and Petrovic 1992; Yan et al. 2004; Yonenaga 2005). In addition to listing toughness, hardness, modulus and yield stress, Table 1 also presents shear modulus, μ , Poisson's ratio, ν , and Burgers vectors, b , for the most likely slip system. Yield strengths are presented both as the hardness conversion, $H/3$, and as a shear yield, $\tau_{ys} = 2\sigma_{ys}/3$, following Johnson (1987) as the maximum reduced stress criterion. The last column, $(\mu\sigma_{ys}b)^{1/2}$, represents the correlation function as described below.

First consider a dislocation line of unit length that develops as a result of the shear stress produced by the indenter. It has a force per unit length, F , of

$$F = \tau b, \tag{2}$$

where τ is the resolved shear stress on the slip plane and in the direction of the slip vector with b the Burgers vector. Since the corners of a Vickers or Berkovich diamond are generally the stress concentration that initiates fracture, one can also assume that this will generally favor dislocation nucleation. The assumption is that emitted dislocations represent a back force on the indenter tip that is nucleating them. As the crack begins to nucleate, these same dislocations represent a back force on the emerging crack nucleus. As N dislocations have been emitted prior to crack extension, the resistive force per unit length on the crack tip is

$$F_R = N\tau b. \tag{3}$$

To first order this represents dislocation shielding.

Next consider the extension force on the putative crack. Assuming that the crack front is subjected to pure mode-II deformation, the extension force is equal to the strain energy release rate, G_{IIc} , as given by

$$G_{IIc} = (1 - \nu^2) \frac{\tau^2 \pi a}{E} = (1 - \nu^2) \frac{K_{IIc}^2}{E}, \quad (4)$$

where the Poisson's ratio term, $(1 - \nu^2)$ represents plane strain conditions. Here E is the elastic modulus, a is the crack length and τ is the applied stress. It is assumed that the crack front is of unit length thereby giving Eq. 4 in units of an extension force per unit length of crack front. At instability, the first order correlation function is found by equating Eqs. 3 and 4, i.e., the crack extension force is equal to the dislocation resistive force. Using the isotropic relationship between Young's and shear moduli of $E = 2\mu(1 + \nu)$, converting shear to uniaxial yield stress, and substituting the experimentally validated theoretical relation between mode-II and mode-I fracture toughness, $K_{Ic} \approx (2/\sqrt{3}) K_{IIc}$,

$$K_{Ic} = \frac{4}{3} \sqrt{\frac{N\mu\sigma_{ys}b}{(1 - \nu)}}. \quad (5)$$

For the correlation function, the relatively constant term $(4/3) \sqrt{N/(1 - \nu)}$ is left out and the result in Fig. 1 gives an exceptional correlation for 22 semiconductor, oxide, carbide, silicide and nitride data including diamond. The correlation covers more than an order of magnitude of fracture toughness values, which represents more than two orders of magnitude in crack extension force as seen from Eq. 4. Furthermore, the line is nearly the best fit linear relationship for Eq. 5 when one assumes $(4/3) \sqrt{N/(1 - \nu)}$ to be constant for these materials. While this might not seem so realistic for the nitrides and diamond, extensive plasticity under indentation of single crystals has been seen in SiC (Page et al. 1998), MoSi₂ (Boldt et al. 1992), MgO (Drory et al. 1996) and the semiconductors. For the six intermetallics, the yield strengths are considerably less and the plasticity greater for equivalent strengths giving rise to larger fracture toughness values. The mean yield strength of the intermetallics was 0.9 GPa while that of the more brittle material was 3.9 GPa discounting diamond. With a greater value for $(4/3) \sqrt{N/(1 - \nu)}$, one can also fit Eq. 5 through the intermetallic data although the scatter precludes a definitive functional relationship. Ignoring the $4/(3\sqrt{1 - \nu})$ term for the moment, to arrive at the linear correlations of Eq. 5

in Fig. 1, the values of N are 808 for the intermetallics and 12 for the more brittle materials. It is significant that this number of 808 shielding dislocations for the intermetallic fit represents an average fracture toughness of 3.6 MPa m^{1/2}. In an earlier study (Huang and Gerberich 1992) of a large grained, thin film Fe-Si alloy, transmission electron microscopy in situ loading led to an applied stress intensity of 4 MPa m^{1/2}. An exact solution of the number of shielding dislocations was obtained. This calculation gave 950 dislocations while the number observed in the transmission electron microscope under load was 1178. Given that N is in the square root of Eq. 5, either of these values would only shift the curve negligibly compared to the data scatter. Additional data on intermetallics would be appropriate as the current scatter does not dictate a definitive slope. However, it is emphasized that this correlation is predominantly based upon the fact that in indentation, dislocation nucleation preceded cracking and hence fracture toughness. Such a correlation may not be as robust in fracture induced by other states of stress.

Validation of the correlation function represented by Eq. 5 is possible by considering dislocation-shielding models. One such model (Huang and Gerberich 1992) utilized both Li's (1986) and Thomson's (1986) analysis of equilibrium dislocation arrays to evaluate the grain size effect on brittle fracture. This gave

$$K_{Ic} \simeq \tau_f \sqrt{\frac{d}{\pi}} + \frac{\mu N b}{4(1 - \nu) \sqrt{d}}, \quad (6)$$

where d is the grain size and the first term involves the friction stress, while the second is the dislocation shielding term. Equation 6 was applied to the intermetallic Ni₃Sn₄ having a mean grain diameter of 32 μm (Ghosh 2004). To shift the correlation line of Fig. 1 to Ni₃Sn₄, the value of N would have to be 640. Using this in Eq. 6, the calculated value of K_{Ic} was 4.36 MPa m^{1/2} compared to the measured value of 4.2 MPa m^{1/2}. It should be mentioned that the length scale for single crystals would be the plastic zone size which is 2.12 times the contact radius (Johnson 1987) rather than the grain size. From this one can eventually show that hardness is proportional to fracture toughness to first order.

Returning to the original premise that dislocation activity precedes fracture and provides dislocation shielding, one should be able to demonstrate that $G_{Ic} > 2\gamma_s$ where γ_s is the surface energy. One could argue that many of the K_{Ic} values converted to G_{Ic} via Eq. 4 are equal to $2\gamma_s$ rather than being greater by treat-

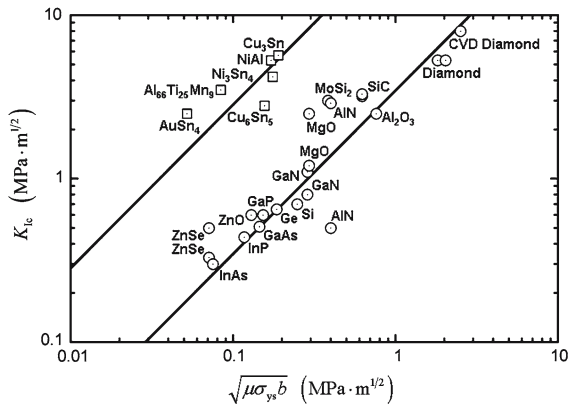


Fig. 1 The proposed model is consistent with 22 relatively brittle materials. The average yield strength of the 6 intermetallics (open squares) was 0.9 GPa, while their average fracture toughness was 3.6 MPa m^{1/2}. Ignoring the Poisson’s factor, the number of dislocations, *N*, necessary for the intermetallic fit was 808. The average yield strength of the more brittle material (open circles) was 3.9 GPa discounting diamond. The number of dislocations necessary for this fit was 12

ing G_{IC} as $2\gamma_{eff}$, where γ_{eff} is equal to γ_s as reported by Messmer and Bilello (Messmer and Bilello 1981). For GaAs, using a sessile drop experiment in vacuum (Kota et al. 2006), the value of γ_s is 0.45 J/m² compared to the value of γ_{eff} equal to 0.9 J/m² taken from fracture experiments (Messmer and Bilello 1981). Similarly, for CdTe γ_{eff} is 1.0 J/m² (Mecholsky 2006) while the sessile drop experiment gave γ_s to be 0.18 J/m² (Kota et al. 2006). For much harder materials such as diamond, the values of Table 1 give γ_{eff} to be 15–30 J/m² while a pseudopotential calculation gave γ_s of 5 J/m² (Hong and Chou 1998). This strongly suggests that for the brittle materials of the lower data set in Fig. 1, that γ_{eff} can be 2 to 5 times as large as the true surface energy. In summary, a correlation with theoretical underpinnings couples fracture toughness and hardness (yield strength) in a broad array of materials subjected to sharp contacts. It is suggested that this may lead to a more in-depth understanding of friction and wear in high hardness materials.

Acknowledgements This research was funded through NSF grant number CMS-0322436.

References

Anstis GR, Chantikul P, Lawn BR, Marshall DB (1981) A critical evaluation of indentation techniques for measuring frac-

ture toughness. I. Direct crack measurements. *J Am Ceram Soc* 64(9):533–538
 Bates SC (2006) Net shape bulk diamond fabrication. <http://www.tvu.com/PC60diamWeb.htm>. Cited 8 Aug 2007
 Bergmann G, Vehoff H (1995) Effect of environment on the brittle-to-ductile transition of pre-cracked NiAl single and polycrystals. *Mater Sci Eng A* 192/193:309–315
 Boldt PH, Embury JD, Weatherly GC (1992) Room temperature microindentation of single-crystal MoSi₂. *Mater Sci Eng A* 155(1–2):251–258
 Burns SJ (1986) Crack tip dislocation nucleation observations in bulk specimens. *Scripta Metall* 20(11):1489–1494
 Cross GLW, Schirmaisen A, Grutter P, Durig UT (2006) Plasticity, healing and shakedown in sharp-asperity nanoindentation. *Nat Mater* 5(5):370–376
 Deneen Nowak J, Mook WM, Minor AM, Gerberich WW, Carter CB (2007) Fracturing a nanoparticle. *Philos Mag* 87(1):29–37
 Drory MD, Gardinier CF, Speck JS (1991) Fracture toughness of chemically vapor-deposited diamond. *J Am Ceram Soc* 74(12):3148–3150
 Drory MD, Ager JW III, Suski T, Grzegory I, Porowski S (1996) Hardness and fracture toughness of bulk single crystal gallium nitride. *Appl Phys Lett* 69(26):4044–4046
 Espinosa HD, Peng B, Moldovan N, Friedmann TA, Xiao X, Mancini DC, Auciello O, Carlisle J, Zorman CA, Merhegany M (2006) Elasticity, strength, and toughness of single crystal silicon carbide, ultrananocrystalline diamond, and hydrogen-free tetrahedral amorphous carbon. *Appl Phys Lett* 89(7):73111
 Evans AG, Charles EA (1976) Fracture toughness determinations by indentation. *J Am Ceram Soc* 59(7–8):371–372
 Gerberich WW, Venkataraman SK, Hoehn JW, Marsh PG (1993) Fracture Toughness of intermetallics using a micro-mechanical probe. *Proc First Int Symp Struct Intermet*, TMS, Warrendale, PA, pp 569–590
 Gerberich WW, Jungk JM, Mook WM (2003a) Crack dislocation interactions. In: Gerberich WW (ed) *Encyclopedia of comprehensive structural integrity*, vol 8. Elsevier, pp 357–382
 Gerberich WW, Mook WM, Perrey CR, Carter CB, Baskes MI, Mukherjee R, Gidwani A, Heberlein J, McMurry PH, Girschick SL (2003b) Superhard silicon nanospheres. *J Mech Phys Solids* 51(6):979–992
 Gerberich WW, Mook WM, Cordill MJ, Jungk JM, Boyce B, Friedmann T, Moody NR, Yang D (2006) Nanoprobng fracture length scales. *Int J Fract* 138(1–4):75–100
 Ghosh G (2004) Elastic properties, hardness, and indentation fracture toughness of intermetallics relevant to electronic packaging. *J Mater Res* 19(5):1439–1454
 Hong S, Chou MY (1998) Effect of hydrogen on the surface-energy anisotropy of diamond and silicon. *Phys Rev B: Condens Matter* 57(11):6262
 Huang H, Gerberich WW (1992) Crack-tip dislocation emission arrangements for equilibrium. II. Comparisons to analytical and computer simulation models. *Acta Metall Mater* 40(11):2873–2881
 Johnson KL (1987) *Contact mechanics*. Cambridge University Press, New York, pp 154–155
 Kitano K, Pollock TM (1993) The kinetics of low temperature deformation in NiAl single crystals. In: *Proc first int symp struct intermet*, TMS, Warrendale, PA, pp 591–599

- Klose FB, Harms U, Neuhauser H, Bakin A, Behrens I, Peiner E, Wehmann HH, Schlachetzki A, Rosler J (2002) Elastic and anelastic properties of Fe-doped InP films on silicon cantilevers. *J Appl Phys* 91(11):9031–9038
- Kota AK, Anand G, Ramakrishnan S, Regel LL, Wilcox WR (2006) Influence of oxygen, hydrogen, helium, argon and vacuum on the surface behavior of molten InSb, other semiconductors, and metals on silica. *J Cryst Growth* 290(2):319–333
- Kumar KS (1993) Microstructure and mechanical properties of ternary Li₂ aluminum-rich intermetallics. In: Proc first int symp struct intermet, TMS, Warrendale, PA, pp 87–96
- Lawn B, Wilshaw R (1975) Indentation fracture: principles and applications. *J Mater Sci* 10(6):1049–1081
- Li JCM (1986) Computer simulation of dislocations emitted from a crack. *Scripta Metall* 20(11):1477–1482
- Lin IH, Thomson R (1986) Cleavage, dislocation emission, and shielding for cracks under general loading. *Acta Metall* 34(2):187–206
- Louail L, Maouche D, Hachemi A (2006) Elastic properties of InAs under pressure up to 18 GPa. *Mater Lett* 60(27):3269–3271
- Margevicius RW, Gumbsch P (1998) Influence of crack propagation direction on {110} fracture toughness of gallium arsenide. *Phil Mag A* 78(3):567–581
- Mecholsky JJ Jr (2006) Estimating theoretical strength of brittle materials using fractal geometry. *Mater Lett* 60(20):2485–2488
- Mecholsky JJ Jr, Freimam SW, Rice RW (1976) Fracture surface analysis of ceramics. *J Mater Sci* 11(7):1310–1319
- Messmer C, Bilello JC (1981) The surface energy of Si, GaAs, and GaP. *J Appl Phys* 52(7):4623–4629
- Minor AM, Lilleodden ET, Jin M, Stach EA, Chrzan DC, Morris JW Jr (2005) Room temperature dislocation plasticity in silicon. *Philos Mag* 85(2–3):323–330
- Minor AM, Syed Asif SA, Zhiwei S, Stach EA, Cyrankowski E, Wyrobek TJ, Warren OL (2006) A new view of the onset of plasticity during the nanoindentation of aluminium. *Nat Mater* 5(9):697–702
- Moody NR, Jungk JM, Mayer TM, Wind RA, George SM (2006) Properties and fracture of tungsten–alumina atomic layer deposited nanolaminates. Eleventh International Conference on Fracture, Paper 5518
- Page TF, Riester L, Hainsworth SV (1998) The plasticity response of 6H-SiC and related isostructural materials to nanoindentation: slip vs. densification. *Mater Res Soc Symp Proc, Mater Res Soc* 522:113–118
- Ruoff AL (1979) On the yield strength of diamond. *J Appl Phys* 50(5):3354–3356
- Terao R, Tatami J, Meguro T, Komeya K (2002) Fracture behavior of AlN ceramics with rare earth oxides. *J Eur Ceram Soc* 22(7):1051–1059
- Veprék S, Argon AS (2002) Towards the understanding of mechanical properties of super- and ultrahard nanocomposites. *J Vac Technol B* 20(2):650–664
- Wade RK, Petrovic JJ (1992) Fracture modes in MoSi₂. *J Am Ceram Soc* 75(6):1682–1684
- Yan C-S, Mao H-K, Li W, Qian J, Zhao Y, Hemley RJ (2004) Ultrahard diamond single crystals from chemical vapor deposition. *Phys Status Solidi A* 201(4):25–27
- Yonenaga I (2005) Hardness, yield strength, and dislocation velocity in elemental and compound semiconductors. *Mater Trans* 46(9):1979–1985